Received: 21 March 2021 | Revised: 26 April 2021 | Accepted: 14 May 2021

DOI: 10.1002/qua.26750

FULL PAPER

International Journal of Quantum Chemistry WILEY

Topological aspects of cavity-induced degeneracies in polyatomic molecules

Péter Badankó[1] | Otabek Umarov[1] | Csaba Fábri[2,3] | Gábor J. Halász[4] | Ágnes Vibók[1,5]

[1]Department of Theoretical Physics, University of Debrecen, Debrecen, Hungary

[2]Laboratory of Molecular Structure and Dynamics, Institute of Chemistry, Eötvös Loránd University, Budapest, Hungary

[3]MTA-ELTE Complex Chemical Systems Research Group, Budapest, Hungary

[4]Department of Information Technology, University of Debrecen, Debrecen, Hungary

[5]ELI-ALPS, ELI-HU Non-Profit Ltd, Szeged, Hungary

Correspondence
Ágnes Vibók, Department of Theoretical Physics, University of Debrecen, PO Box 400, H-4002 Debrecen, Hungary.
Email: vibok@phys.unideb.hu

Funding information
EU-funded Hungarian grant, Grant/Award Number: EFOP-3.6.2-16-2017-00005; NKFIH, Grant/Award Number: K128396

Abstract

Conical intersections are degeneracies between multidimensional potential energy surfaces of molecular systems. It is well known that, besides these phenomena significantly modify the spectroscopic and dynamical properties of molecules, their presence in a molecular system has noticeable topological implications, as well. Such a consequence is the appearance of the topological or geometric phase. Conical intersections not only occur in nature but they can also be created by light. This can either be classical laser light or quantum light in an optical cavity. As a showcase example, by placing the formaldehyde (H_2CO) molecule into a cavity, the topological properties (e.g., geometric or Berry phase) of the emerging light-induced conical intersection have been investigated for different cavity parameters and geometrical arrangements.

KEYWORDS
Born–Oppenheimer approximation, geometric phase effect, nonadiabatic coupling, cavity-induced conical intersections, polaritons

1 | INTRODUCTION

The Born–Oppenheimer (BO) approximation [1, 2] is one of the fundamental approximations of atomic and molecular physics. It is based on the fact that the heavy nuclei move much slower than the light electrons, which makes it possible to separate their motions and treat them separately. However, there are processes,—such as ultrafast radiationless relaxation, photodissociation, photofragmentation, chemiluminescence or isomerization of polyatomic molecules and so forth…—which are among the intensively studied areas of today's physical chemistry [3–8] where the BO approximation loses its validity. In these processes the nuclear vibrations and the electronic degrees of freedom cannot be treated separately as they are strongly coupled providing so-called conical intersections (CIs), which can form highly efficient pathways for a significant energy exchange between the nuclei and electrons [3–8]. The nonadiabatic coupling (NAC) that can couple the various electronic states of the molecule is singular (as is well known from the Hellman–Feynman theorem) at the degeneracy points resulting in remarkable changes in the dynamical, spectroscopic [9–14] and topological properties. For example, topological effects give rise to a number of interesting subjects [15–24] like the phenomena of Longuet-Higgins or Berry phase, the quantization feature of the NACs, the existence of molecular field and the topological spin and so forth… From now on we call the naturally occurring CIs, which are entirely inherent attributes of polyatomic molecules, "natural" or "intrinsic" CIs.

Nonadiabatic phenomena can also be created when the molecule is exposed to laser light and so-called light-induced conical intersections (LICIs) are formed. In the last decade vast number of theoretical and experimental works have been devoted to this subject. Most of them have

focused on diatomic molecules [25–40], but there are quite a lot of polyatomic results as well [41–46], that clearly demonstrate how the LICIs can affect and control the different spectroscopic and molecular dynamic properties. Among these studies, the topological consequences of light-induced nonadiabaticity have also been investigated, both in time-independent [26, 27] and time-dependent adiabatic [36] pictures.

Light-induced nonadiabatic phenomena can also be induced if classical laser light is replaced by the quantized electric field of an optical or plasmonic nanocavity. The confined photonic mode of the cavity can resonantly couple the electronic states of the molecule, which gives rise to mixed polaritonic states carrying both photonic and excitonic features. It is known today that these hybrid light-matter polaritonic states can dramatically modify the different dynamical, kinetical and spectroscopic and so forth… properties of the molecular systems [34, 47–56]. These important findings mark the birth of polaritonic chemistry, a novel field of research in physical chemistry. Obviously, the field-free topological features are also highly affected by the light-matter interaction, which is manifested, for example, in the position change of the natural CIs (if they are present in the system) or in the emergence of some novel topological properties like formation of a polaritonic LICI. A recent paper [38] has investigated the topological properties of polaritonic LICIs in the diatomic LiF molecule. In this case, in addition to the single vibrational nuclear coordinate, a rotational degree of freedom brought into play by the cavity provides the second degree of freedom that, together with the internuclear distance, span the branching space in which the degeneracy is lifted. However, in contrast to diatomics, polyatomic molecules possess enough vibrational degrees of freedom to form LICIs without the inclusion of any rotational degrees of freedom. As such studies for polyatomic molecules have not been performed yet, we set the goal of studying polaritonic LICIs in the space of vibrational modes of polyatomic molecules.

The purpose of the present work is to perform topological or Berry phase investigations of a LICI which is formed between two polaritonic states in the polyatomic formaldehyde (H_2CO) molecule, by means of incorporating the calculation of adiabatic-to-diabatic transformation (ADT) angles with the time-independent line integral approach [8]. This molecule can be considered as an appropriate candidate to study the consequences of light-induced nonadiabaticity because it not only lacks a natural CI in the vicinity of the Franck–Condon (FC) region, but also does not have any first-order NAC between the ground and first singlet excited electronic states around its equilibrium geometry [57–59].

The article is organized as follows. In the next section, the working Hamiltonian, as well as the numerical procedures are briefly summarized. Then the applied method and the basic formulae, as well as the numerical results are presented and discussed. Finally we present conclusions in the last section.

2 | THE WORKING HAMILTONIAN

The Hamiltonian of a molecule coupled to a single cavity mode can be written as

$$\hat{H}_{\mathrm{mc}} = \hat{H}_0 + \hbar\omega_{\mathrm{c}}\hat{a}^{\dagger}\hat{a} - g\hat{\vec{\mu}}\,\vec{e}\left(\hat{a}^{\dagger} + \hat{a}\right) \tag{1}$$

where $\hat{H}_0$ denotes the Hamiltonian of the isolated molecule, $\hat{a}^{\dagger}$, $\hat{a}$ and ω_{c} correspond to the creation and annihilation operators and the angular frequency of the cavity mode, respectively, g is the coupling strength parameter, $\hat{\vec{\mu}}$ is the electric dipole moment operator of the molecule and $\vec{e}$ is the polarization vector of the cavity mode. If the two singlet electronic states $S_0\left(\tilde{X}^1A_1\right)$ and $S_1\left(\tilde{A}^1A_2\right)$ of H_2CO are taken into account, the matrix representation of $\hat{H}_{\mathrm{mc}}$ in the direct product basis of the two electronic states and Fock states $|n\rangle$ ($n = 0, 1, 2, \ldots$) of the cavity mode has the form

$$\hat{H} = \begin{bmatrix} \hat{T}+V_{\mathrm{X}} & 0 & W_1^{\mathrm{X}} & W_1 & 0 & 0 & \ldots \\ 0 & \hat{T}+V_{\mathrm{A}} & W_1 & W_1^{\mathrm{A}} & 0 & 0 & \ldots \\ W_1^{\mathrm{X}} & W_1 & \hat{T}+V_{\mathrm{X}}+\hbar\omega_{\mathrm{c}} & 0 & W_2^{\mathrm{X}} & W_2 & \ldots \\ W_1 & W_1^{\mathrm{A}} & 0 & \hat{T}+V_{\mathrm{A}}+\hbar\omega_{\mathrm{c}} & W_2 & W_2^{\mathrm{A}} & \ldots \\ 0 & 0 & W_2^{\mathrm{X}} & W_2 & \hat{T}+V_{\mathrm{X}}+2\hbar\omega_{\mathrm{c}} & 0 & \ldots \\ 0 & 0 & W_2 & W_2^{\mathrm{A}} & 0 & \hat{T}+V_{\mathrm{A}}+2\hbar\omega_{\mathrm{c}} & \ldots \\ \vdots & \vdots & \vdots & \vdots & \vdots & \vdots & \ddots \end{bmatrix} \tag{2}$$

where $\hat{T}$ is the kinetic energy operator, V_{X} and V_{A} denote the ground-state and excited-state potential energy surfaces (PESs) and $W_n = -g\sqrt{n}\vec{d}\vec{e}$ where $\vec{d}$ is the transition dipole moment (TDM) vector. $W_n^{\mathrm{X}} = -g\sqrt{n}\vec{d}_{\mathrm{X}}\vec{e}$ and $W_n^{\mathrm{A}} = -g\sqrt{n}\vec{d}_{\mathrm{A}}\vec{e}$ where $\vec{d}_{\mathrm{X}}$ and $\vec{d}_{\mathrm{A}}$ refer to the permanent dipole moments (PDMs) associated with the electronic states X and A, respectively. The polaritonic (adiabatic) PESs (PoPESs) can be obtained as eigenvalues of the potential energy part (i.e., $\hat{H} - \hat{T}\mathbf{I}$ where $\mathbf{I}$ refers to the identity matrix of appropriate dimension) of the Hamiltonian of Equation (2) at each nuclear configuration.

The planar equilibrium structure of H_2CO (C_{2v} symmetry) in its ground electronic state (X) and its normal modes with characterization and C_{2v} symmetry labels are shown in Figure 1. The excited electronic state (A) has a double-well structure along the ν_4 (out-of-plane bend) vibrational mode and the two equivalent nonplanar equilibrium structures (C_s symmetry) are connected by a planar transition state structure (C_{2v} symmetry). Due to symmetry, all components of the TDM vanish at geometries of C_{2v} symmetry.

In this study the two-dimensional 2D (ν_2, ν_4) computational model, treating the ν_2 (C=O stretch) and ν_4 (out-of-plane bend) vibrational modes, was used. First, normal coordinates at the planar transition state structure of the A electronic state were evaluated. Then, the four inactive normal coordinates (modes ν_1, ν_3, ν_5 and ν_6) were set to zero, PES (V_X and V_A) and TDM values were calculated at the CAM-B3LYP/6-31G* level of theory by making displacements along the ν_2 and ν_4 modes and the resulting PES and TDM data points were interpolated. In the 2D (ν_2, ν_4) model, only the body-fixed y component of the TDM (B_1 symmetry) can be nonzero and the PDM vector is perpendicular to the TDM vector.

Equation (2) provides the expression for the diabatic Hamiltonian. Neglecting the permanent dipoles and the off-resonant couplings one can transform the diabatic Hamiltonian into the adiabatic picture. To obtain the PoPES $V^{\text{lower}}_{\text{PoPES}}(Q_2, Q_4)$ and $V^{\text{upper}}_{\text{PoPES}}(Q_2, Q_4)$ it is sufficient to diagonalize the two-dimensional PES matrix

$$\begin{bmatrix} V_A & W_1 \\ W_1 & V_X + \hbar\omega_c \end{bmatrix} \tag{3}$$

which corresponds to the so-called singly-excited subspace (excited electronic state with zero photon and ground electronic state with one photon). These two PoPESs can cross each other, forming a LICI, only if the two conditions $Q_4 = 0$ and $V_X\left(Q_2^{\text{CI}}; Q_4 = 0\right) = V_A\left(Q_2^{\text{CI}}; Q_4 = 0\right) - \hbar\omega_c$ are simultaneously fulfilled (see in Figure 2). In this case, the branching space is spanned by the vibrational modes ν_2 (A_1 symmetry) and ν_4 (B_1 symmetry) such that ν_2 is the tuning mode and ν_4 is the coupling mode.

3 | RESULTS AND DISCUSSIONS

The adiabatic Hamiltonian (we can call it polaritonic Hamiltonian) lacks of cavity couplings in its potential energy part because the coupling terms are transformed into the kinetic energy part of the Hamiltonian matrix as momentum couplings. We can calculate the NAC terms between the second and third (lower and upper) polaritonic states as the derivatives of the transformation angle Φ of the ADT matrix with respect to the corresponding nuclear degrees of freedom ($\tau_{23Q_4} = \partial\Phi/\partial Q_4$ and $\tau_{23Q_2} = \partial\Phi/\partial Q_2$). In Figure 3 the NAC terms, as well as the absolute value of the NAC vector in the close vicinity of the LICI are visualized. The latter is defined as follows:

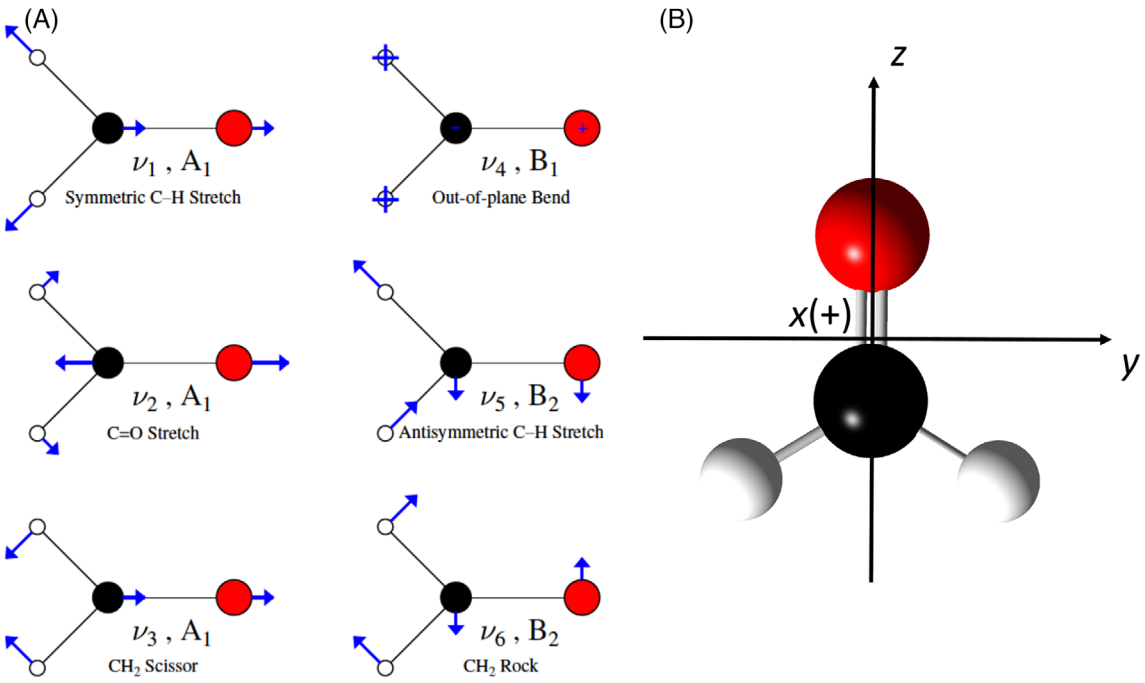

FIGURE 1 Normal modes with C_{2v} symmetry labels (panel A) and equilibrium structure (panel B) of H_2CO in its ground electronic state. The definition of the body-fixed coordinate axes is shown in panel B (the x axis is directed outwards, as indicated by the + sign)

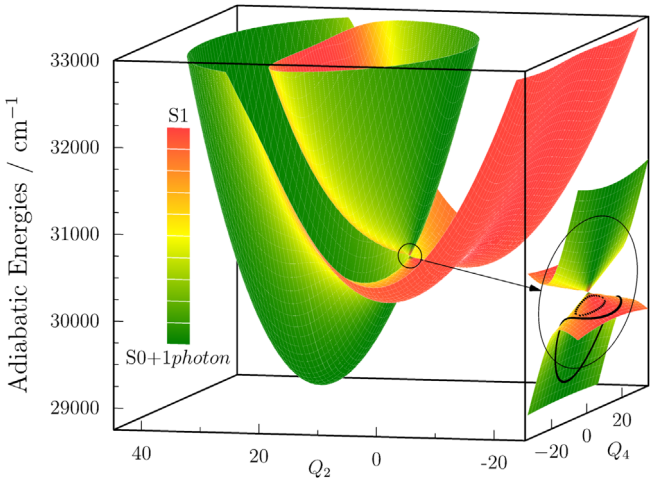

FIGURE 2 The second and third lowest polaritonic (adiabatic) surfaces of the formaldehyde molecule coupled to a single cavity mode. Q_2 and Q_4 are the normal coordinates of the ν_2 (C═O stretch) and ν_4 (out-of-plane bend) vibrational modes. The cavity frequency and coupling strength values are $\omega_c = 29\,000\ \text{cm}^{-1}$ and $g = 5.34 \times 10^{-2}$ au, respectively. The polaritonic light-induced conical intersection (LICI) between the second and third polaritonic surfaces is displayed in the inset. The two different closed contours applied in the topological phase calculations are also displayed in the inset. The character of the PoPESs is indicated by different colors (see the legend on the left; the labels S_0 and S_1 refer to the ground and excited electronic states of the molecule)

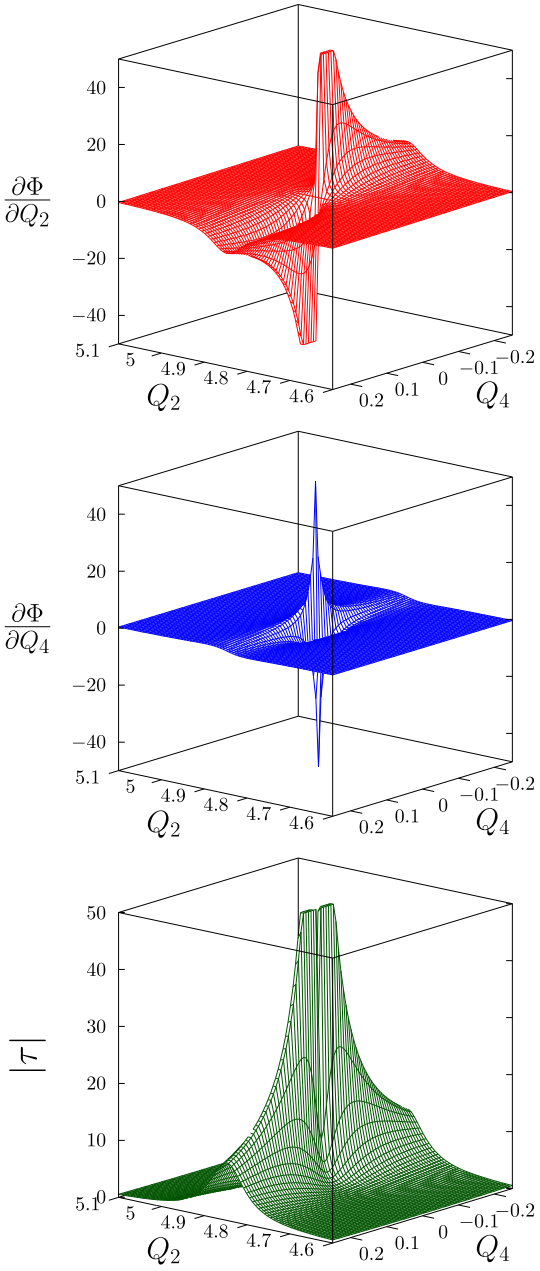

FIGURE 3 The nonadiabatic coupling terms: $\tau_{23Q_2} = \partial\Phi/\partial Q_2$ and $\tau_{23Q_4} = \partial\Phi/\partial Q_4$, as well as their absolute value ($|\tau_{23}| = \sqrt{\tau^2_{23Q_2} + \tau^2_{23Q_4}}$) for H_2CO, in top, middle and bottom panels, respectively. The applied coupling strength and cavity frequency are $g = 5.34 \times 10^{-2}$ au and $\omega_c = 29\,000\,\text{cm}^{-1}$, respectively

$$|\tau_{23}| = \sqrt{\tau^2_{23Q_2} + \tau^2_{23Q_4}}. \tag{4}$$

Here the applied cavity coupling strength and frequency are chosen as $g = 5.34 \times 10^{-2}$ au and $\omega_c = 29\,000$ cm^{-1}, respectively. Similarly to the magnitude of natural NAC in polyatomic molecules, the light-induced NAC terms can be extremely large, in fact singular, at the polaritonic LICI configuration.

As a next step we consider the topological properties of the polyatomic polaritonic LICI and calculate its geometric phase. First, we review the results of Longuet-Higgins and Herzberg [15, 16] who demonstrated that each real-valued field-free adiabatic electronic state changes sign when transported continuously along a closed loop surrounding the point of degeneracy. Next, Mead and Truhlar combined the subject of geometric phase with the single electronic state problem [17] and Berry provided a general interpretation of the theory [18]. Therefore the name is termed as "Berry phase," which has become a pivotal subject in several fields of chemistry and physics. One of the clearest observable manifestations of the topological phase is the ordering of the vibronic energy levels in molecular systems [60, 61]. Moreover, it was shown that the topological phase is gauge invariant [62–64], therefore it is a measurable quantity. In fact, the existence of the Berry phase was also confirmed experimentally [65, 66].

Since the total molecular wave function has to be single valued, it is preferential to make the adiabatic polaritonic wave function complex by multiplying it with a phase factor, preserving the single valuedness of the total molecular wave function. This amendment of the polaritonic eigenfunctions has a direct impact on nuclear dynamics even in a single PoPES situation. Consequently, the emergence of the Berry phase in a molecular system can be seen as an obvious fingerprint of the CI no matter whether it is natural or cavity-induced.

So as to calculate the topological or Berry phase α_{23}, similarly to the field-free situation [26, 27], we resort to the line integral technique. It is know from the earlier works of Baer [5, 8] that the line integral value of the NAC vector along a contour Γ in the configuration space is equal to the ADT angle

$$\gamma_{23}(\Gamma) = \int_\Gamma \tau_{23}(s') \cdot ds'. \tag{5}$$

If we consider a closed contour Γ, we can obtain the topological or Berry phase α_{23}

$$\alpha_{23} = \oint_\Gamma \tau_{23}(s') \cdot ds', \tag{6}$$

where τ_{23} is the NAC term of Equation (5) between the second and third (lower and upper) PoPESs. The consequence of the sign change of the polaritonic wave function is that the value of α_{23} equals

$$\alpha_{23} = \pi \times \begin{cases} 2n+1 & \text{if } \Gamma \text{ encompasses odd number of CIs} \\ 2n & \text{if } \Gamma \text{ encompasses even number of CIs} \end{cases} \qquad n = 0, \pm 1, \pm 2, \ldots \tag{7}$$

Let us consider now the technical aspects of the calculation of the topological phase. In the inset of Figure 2 the LICI is visualized between the second and third PoPES over the branching space (Q_2, Q_4). The geometrical layout for the topological phase calculations is presented in Figure 4 (middle panel). In Figure 4 two different closed contours are defined over the configuration space, but only one of them encircles the polaritonic LICI. One can perform numerical simulations along these closed contours which are labeled with their centers (Q_2^0, Q_4^0) and "radii" ρ_i. The actual position is determined by an angle $\varphi \in [0, 2\pi]$:

$$\begin{aligned} Q_2 &= Q_2^0 + \rho_2 \cos\varphi \\ Q_4 &= Q_4^0 + \rho_4 \sin\varphi. \end{aligned} \tag{8}$$

In Figure 4 (middle panel) the obtained values of the γ_{23} transformation angle are shown for the two different paths P_0 and P_1, as well as three different cavity coupling strengths ($g = 5.34 \times 10^{-3}$ au, $g = 5.34 \times 10^{-2}$ au and $g = 5.34 \times 10^{-1}$ au), respectively. It is well noticeable that α_{23} differs from zero only in that case when the closed path encircles the LICI. In this situation we get $\alpha_{23} = -\pi$, regardless of the applied cavity coupling strength. In case of small cavity coupling strength, if the value of Q_2 is significantly greater than the value of Q_2^{CI}, the adiabatic and diabatic states are approximately the same, therefore the value of the ADT angle is $\Phi \approx k \times \pi$. If the value of Q_2 is less than Q_2^{CI}, then the adiabatic states are almost identical to the diabatic ones, they are just swapped, therefore the value of the ADT angle is approximately equal to $(k + 1/2) \times \pi$.

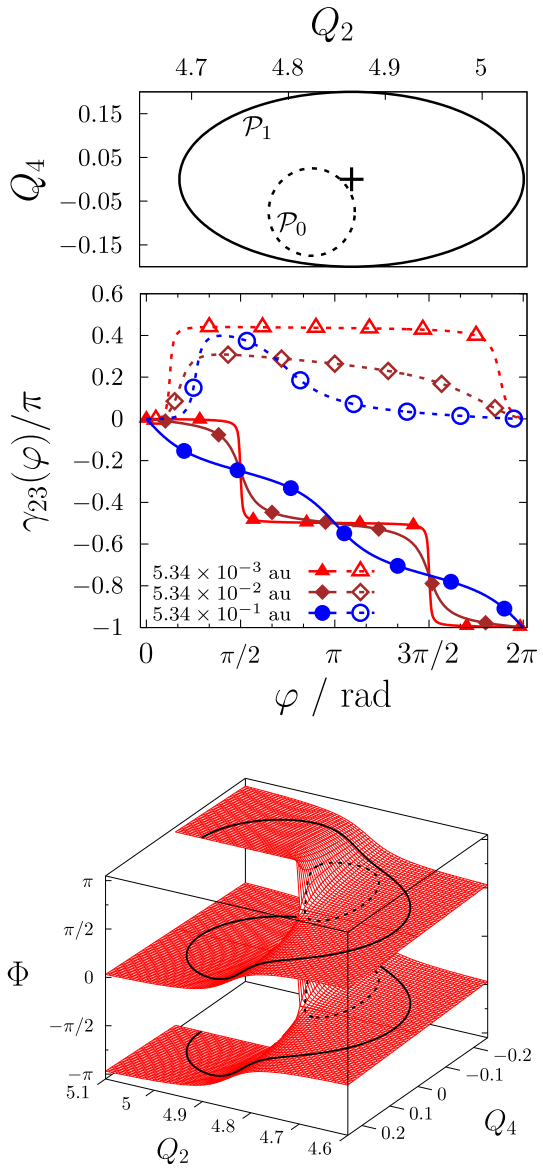

FIGURE 4 Geometrical arrangement of the different contours applied in the geometric phase calculations. Two different paths P_0 and P_1 are presented but only one of them (P_1) surrounds the light-induced conical intersection (LICI) (top panel). Line integral of the NACs as a function of the position along the two different studied circles (middle panel). The curves marked by filled markers are calculated along a contour surrounding the LICI. Three different coupling strengths ($g = 5.34 \times 10^{-3}$ au, $g = 5.34 \times 10^{-2}$ au, $g = 5.34 \times 10^{-1}$ au) and one cavity frequency ($\omega_c = 29\,000$ cm^{-1}) are applied. Three dimensional plots of the transformation angle as multivalued functions of Q_2 and Q_4 (bottom panel) are presented ($g = 5.34 \times 10^{-2}$ au and $\omega_c = 29\,000$ cm^{-1})

Finally, when Q_2 almost coincides with Q_2^{CI}, the two states are strongly mixed and sharp steps appear in the γ_{23} curve (see at $\varphi = \pi/2$ and $\varphi = 3\pi/2$ in the middle panel of Figure 4). This effect becomes more and more blurred as the intensity increases since the states are mixed over an increasingly wider range, which leads to smoothing out the steps. The trace of this effect is clearly visible in the continuous curves of the middle panel of Figure 4. If a contour does not surround the polaritonic LICI, the topological phase takes the value $\alpha_{23} = 0$ for all coupling strengths. It is expected that a significant change in the value of the ADT angle occurs near the position of the LICI. Yet, it is eye-catching, that the different curves give rise to different shapes of the NAC vectors, which display sudden jumps along the contour (see in Figure 4 middle panel, dashed curves). The numerical results obtained fully corroborate the statement of Equation (7).

To better understand the numerical results, a three-dimensional figure displays the ADT transformation angle over the (Q_2, Q_4) branching space in the bottom panel of Figure 4 applying the cavity parameters $g = 5.34 \times 10^{-2}$ au and $\omega_c = 29\,000$ cm^{-1}. It is apparent that the curve which does not encircle the LICI closes on its own, while the other curve is shifted by π as surrounding the polaritonic LICI. This shift is closely related to the geometric phase as the geometric phase is obtained as the line integral of the NAC (see Equation 6) whose components are the derivatives of the ADT transformation angle ($\tau_{23Q_i} = \partial\Phi/\partial Q_i$). In other words, when the value of the ADT angle does not change around a closed circle, the line integral value of τ_{23Q_i} should be equal to zero, but when the value of the ADT angle jumps by π, the line integral value of τ_{23Q_i} should be equal to π, as well.

4 | CONCLUSIONS

In this article we have considered the topological consequences of a light-induced CI by placing the formaldehyde molecule into an optical cavity. This molecule lacks a natural CI in the vicinity of the Franck–Condon region and does not possess any first-order NAC between the ground and first singlet excited electronic states around its equilibrium geometry. Therefore, the obtained topological features are unambiguously the fingerprint of light-induced nonadiabatic phenomena which are induced by the cavity quantum light.

Combining the line integral technique with the calculations of the ADT angle results have been presented for the value of the topological phase. Calculation along a closed contour surrounding the LICI provided $\alpha_{23} = \pi$, while the other contour which does not encircle the LICI yielded $\alpha_{23} = 0$ for the value of the topological phase. As known from the natural nonadiabatic phenomena for the situation of "intrinsic" CIs, this result can be considered as a clear evidence that a "true" CI has been found.

In this respect, it can be inferred that the value of the topological phase is independent of whether it is due to a polaritonic LICI or an "intrinsic" CI. The topological phase is determined by whether the closed contour providing the path for the integration in Equation (6) encircles a CI (LICI) or not.

ACKNOWLEDGMENTS

This research was supported by the EU-funded Hungarian grant EFOP-3.6.2-16-2017-00005. The authors are grateful to NKFIH for support (Grant K128396).

AUTHOR CONTRIBUTIONS

Péter Badankó: Validation; writing-original draft. **Otabek Umarov:** Software; validation. **Csaba Fábri:** Writing-original draft. **Gabor Halász:** Supervision; writing-original draft. **Agnes Vibok:** Supervision; writing-original draft.

DATA AVAILABILITY STATEMENT

The data that support the findings of this study are available from the corresponding author upon reasonable request.

ORCID

Ágnes Vibók https://orcid.org/0000-0001-6821-9525

REFERENCES

[1] M. Born, *Ann. Phys.* **1927**, *84*, 457.
[2] J. von Neumann, E. P. Wigner, *Zeit. fur Phys.* **1929**, *30*, 467.
[3] H. Köppel, W. Domcke, L. S. Cederbaum, *Adv. Chem. Phys.* **1984**, *57*, 59.
[4] D. R. Yarkony, *Rev. Mod. Phys.* **1996**, *68*, 985.
[5] M. Baer, *Phys. Rep.* **2000**, *358*, 75.
[6] G. A. Worth, L. S. Cederbaum, *Annu. Rev. Phys. Chem.* **2004**, *55*, 127.
[7] W. Domcke, D. R. Yarkony, H. Köppel, *Conical Intersections: Electronic Structure, Dynamics and Spectroscopy*, World Scientific, Singapore **2004**.
[8] M. Baer, *Beyond Born Oppenheimer: Electronic Non-Adiabatic Coupling Terms and Conical Intersections*, Wiley, Hoboken, NJ **2006**.
[9] C. Xie, J. Ma, X. Zhu, D. R. Yarkony, D. Xie, H. Guo, *J. Am. Chem. Soc.* **2016**, *138*, 7828.
[10] F. E. Curchod Basile, F. Agostini, *J. Phys. Chem. Lett.* **2017**, *8*, 831.
[11] C. Xie, D. R. Yarkony, H. Guo, *Phys. Rev. A* **2017**, *95*, 022104.
[12] C. Xie, B. K. Kendrick, D. R. Yarkony, H. Guo, *J. Chem. Theory Comput.* **2017**, *13*, 1902.
[13] C. Xie, C. L. Malbon, H. Guo, D. R. Yarkony, *Acc. Chem. Res.* **2019**, *52*, 501.
[14] C. Xie, B. Zhao, C. L. Malbon, D. R. Yarkony, D. Xie, H. Guo, *J. Phys. Chem. Lett.* **2020**, *11*, 191.
[15] G. Herzberg, H. C. Longuet-Higgins, *Discuss. Faraday Soc.* **1963**, *35*, 77.
[16] H. C. Longuet-Higgins, *Proc. R Soc. (London) A* **1975**, *344*, 147.
[17] C. A. Mead, D. G. Truhlar, *J. Chem. Phys.* **1979**, *70*, 2284.
[18] M. V. Berry, *Proc. R. Soc. (London) A* **1984**, *392*, 45.
[19] I. G. Ryabinkin, A. F. Izmaylov, *Phys. Rev. Lett.* **2013**, *111*, 220406.
[20] L. Joubert-Doriol, I. G. Ryabinkin, A. F. Izmaylov, *J. Chem. Phys.* **2014**, *140*, 214116.
[21] L. Joubert-Doriol, J. Sivasubramanium, I. G. Ryabinkin, A. F. Izmaylov, *J. Phys. Chem. Lett.* **2017**, *8*, 452.
[22] S. K. Min, A. Abedi, K. S. Kim, E. K. U. Gross, *Phys. Rev. Lett.* **2014**, *113*, 263004.
[23] R. Requist, F. Tandetzky, E. K. U. Gross, *Phys. Rev. A* **2016**, *93*, 042108.
[24] A. Scherrer, F. Agostini, D. Sebastiani, E. K. U. Gross, R. Vuilleumier, *Phys. Rev. X* **2017**, *7*, 031035.
[25] N. Moiseyev, M. Sindelka, L. S. Cederbaum, *J. Phys. B* **2008**, *41*, 221001.
[26] G. J. Halász, Á. Vibók, M. Sindelka, N. Moiseyev, L. S. Cederbaum, *J. Phys. B* **2011**, *44*, 175102.
[27] G. J. Halász, M. Sindelka, N. Moiseyev, L. S. Cederbaum, Á. Vibók, *J. Phys. Chem. A* **2012**, *116*, 2636.
[28] G. J. Halász, Á. Vibók, L. S. Cederbaum, *J. Phys. Chem. Lett.* **2015**, *6*, 348.
[29] A. Natan, M. R. Ware, V. S. Prabhudesai, U. Lev, B. D. Bruner, O. Heber, P. H. Bucksbaum, *Phys. Rev. Lett.* **2016**, *116*, 143004.

[30] A. Csehi, G. J. Halász, L. S. Cederbaum, Á. Vibók, *Faraday Discuss.* **2016**, *194*, 479.
[31] A. Csehi, G. J. Halász, L. S. Cederbaum, Á. Vibók, *J. Phys. Chem. Lett.* **2017**, *8*, 1624.
[32] T. Szidarovszky, G. J. Halász, A. G. Császár, L. S. Cederbaum, Á. Vibók, *J. Phys. Chem. Lett.* **2018**, *9*, 2239.
[33] T. Szidarovszky, G. J. Halász, A. G. Császár, L. S. Cederbaum, Á. Vibók, *J. Phys. Chem. Lett.* **2018**, *9*, 6215.
[34] A. Csehi, M. Kowalewski, G. J. Halász, Á. Vibók, *New J. Phys.* **2019**, *21*, 093040.
[35] M. Pawlak, T. Szidarovszky, G. J. Halász, Á. Vibók, *Phys. Chem. Chem. Phys.* **2020**, *22*, 3715.
[36] G. J. Halász, P. Badankó, Á. Vibók, *Mol. Phys.* **2018**, *116*, 2652.
[37] M. Kübel, M. Spanner, Z. Dube, A. Y. Naumov, S. Chelkowski, A. D. Bandrauk, M. J. J. Vrakking, P. B. Corkum, D. M. Villeneuve, A. Staudte, *Nat. Commun* **2020**, *11*, 1.
[38] M. H. Farag, A. Mandal, P. Huo, chemrxiv.org **2021**.
[39] J. F. Triana, J. L. Sanz-Vicario, *J. Chem. Phys.* **2021**, *154*, 094120.
[40] J. F. Triana, J. L. Sanz-Vicario, *Phys. Rev. Lett.* **2019**, *122*, 063603.
[41] P. V. Demekhin, L. S. Cederbaum, *J. Chem. Phys.* **2013**, *139*, 154314.
[42] J. Kim, H. Tao, J. L. White, V. S. Petrović, T. J. Martinez, P. H. Bucksbaum, *J. Phys. Chem. A* **2012**, *116*, 2758.
[43] M. E. Corrales, J. González-Vázquez, G. Balerdi, I. R. Solá, R. de Nalda, L. Bañares, *Nat. Chem.* **2014**, *6*, 785.
[44] C. Fábri, B. Lasorne, G. J. Halász, L. S. Cederbaum, Á. Vibók, *J. Phys. Chem. Lett.* **2020**, *11*, 5324.
[45] C. Fábri, G. J. Halász, L. S. Cederbaum, Á. Vibók, *Chem. Sci.* **2021**, *12*, 1251.
[46] C. Fábri, B. Lasorne, G. J. Halász, L. S. Cederbaum, Á. Vibók, *J. Chem. Phys.* **2020**, *153*, 234302.
[47] A. Hutchison, T. Schwartz, C. Genet, E. Devaux, T. W. Ebbesen, *Angew. Chem., Int. Ed.* **2012**, *51*, 1592.
[48] J. Galego, F. J. Garcia-Vidal, J. Feist, *Phys. Rev. X* **2015**, *5*, 041022.
[49] M. Kowalewski, K. Bennett, S. Mukamel, *J. Phys. Chem. Lett.* **2016**, *7*, 2050.
[50] R. Chikkaraddy, B. De Nijs, F. Benz, S. J. Barrow, O. A. Scherman, E. Rosta, A. Demetriadou, P. Fox, O. Hess, J. J. Baumberg, *Nature* **2016**, *535*, 127.
[51] R. F. Ribeiro, L. A. Martínez-Martínez, M. Du, J. Campos-Gonzalez-Angulo, J. Yuen-Zhou, *Chem. Sci* **2018**, *9*, 6325.
[52] O. Vendrell, *Phys. Rev. Lett.* **2018**, *121*, 253001.
[53] F. Herrera, J. Owrutsky, *J. Chem. Phys.* **2020**, *152*, 100902.
[54] G. Groenhof, J. J. Toppari, *J. Phys. Chem. Lett.* **2018**, *9*, 4848.
[55] A. Mandal, P. Huo, *J. Phys. Chem. Lett.* **2019**, *10*, 5519.
[56] M. Ruggenthaler, N. Tancogne-Dejean, J. Flick, H. Appel, A. Rubio, *Nat. Rev. Chem.* **2018**, *2*, 0118.
[57] M. Araújo, B. Lasorne, M. J. Bearpark, M. A. Robb, *J. Phys. Chem. A* **2008**, *112*, 7489.
[58] M. Araújo, B. Lasorne, A. L. Magalhães, G. A. Worth, M. J. Bearpark, M. A. Robb, *J. Chem. Phys.* **2009**, *131*, 144301.
[59] M. Araújo, B. Lasorne, A. L. Magalhães, M. J. Bearpark, M. A. Robb, *J. Phys. Chem. A* **2010**, *114*, 12016.
[60] H. Koizumi, I. B. Bersuker, *Phys. Rev. Lett.* **1999**, *83*, 3009.
[61] F. S. Ham, *Phys. Rev. Lett.* **1987**, *78*, 725.
[62] J. Samuel, R. Bhandari, *Phys. Rev. Lett.* **1988**, *60*, 2339.
[63] R. Bhandari, *Phys. Lett. A* **1991**, *157*, 221.
[64] J. Samuel, A. Dhar, *Phys. Rev. Lett.* **2001**, *87*, 260401.
[65] D. Suter, K. T. Mueller, A. Pines, *Phys. Rev. Lett.* **1988**, *60*, 1218.
[66] S. Fuentes-Guridi, S. Bose, V. Vedral, *Phys. Rev. Lett.* **2000**, *85*, 5018.

How to cite this article: P. Badankó, O. Umarov, C. Fábri, G. J. Halász, Á. Vibók, *Int J Quantum Chem* **2021**, e26750. https://doi.org/10.1002/qua.26750